Internal Bond Rotation in Substituted Methyl Radicals, H_2B-CH_2, H_3C-CH_2, H_2N-CH_2, and $HO-CH_2$: Hardness Profiles

Tadafumi Uchimaru,* Asit K. Chandra, Shun-ichi Kawahara, Kazunari Matsumura, Seiji Tsuzuki, and Masuhiro Mikami

Department of Physical Chemistry, National Institute of Materials and Chemical Research, Agency of Industrial Science and Technology, MITI, Tsukuba, Ibaraki 305-8565 Japan

Received: September 13, 2000; In Final Form: December 6, 2000

The energy profiles for the internal bond rotation of substituted methyl radicals, X-CH_2 (X = BH_2, CH_3, NH_2, and OH) were examined with B3LYP/6-31G(d) calculations. Energy evaluation of each point along the rotational coordinate was also carried out with single-point calculation at the computational levels of B3LYP/6-311+G(2df,p) and QCISD(T)/6-311+G(2df,p). The computed rotational energy profiles, as well as the calculated values for the geometrical parameters, the vibrational frequencies, and the ionization potential, were in reasonable agreement with previously reported experimental and theoretical results. Except for H_3C-CH_2 radical, the profiles of chemical potential and hardness along the rotational coordinates present striking contrast to those expected from the corollary of the principle of maximum hardness. Thus, there seems to be no rigorous reason for hardness to be minimum in the transition state region, in general.

1. Introduction

Mulliken[1] and Pearson[2,3] introduced the concept of chemical hardness. Mulliken defined hardness or softness in terms of exchange repulsion energy between acids and bases.[1] Pearson provided a detailed qualitative interpretation of hard and soft behavior of chemical species.[2−4] Hardness (η) is related to electronic chemical potential (μ). The quantitative definitions of μ[5,6] and η[7] have been given as follows:

$$\mu = (\partial E/\partial N)_{v,T} \tag{1a}$$

$$2\eta = (\partial^2 E/\partial N^2)_{v,T} = (\partial \mu/\partial N)_{v,T} \tag{1b}$$

where E and N are the total energy and the number of electrons of the system concerned; the subscripts v and T indicate that external potential (v) and temperature (T) should remain constant. Frequently, three-point finite difference approximation is employed for the energy derivatives, and thus, operational expressions for μ and η are given as follows:[7,8]

$$\mu = -(\mathrm{IP} + \mathrm{EA})/2 \tag{2a}$$

$$\eta = (\mathrm{IP} - \mathrm{EA})/2 \tag{2b}$$

where IP and EA are the first vertical ionization potential and electron affinity, respectively. If Koopmans' approximation is applied to eqs 2, the expressions for μ and η can be written in terms of the energy levels of frontier orbitals, i.e., the highest occupied molecular orbital (HOMO) and the lowest unoccupied molecular orbital (LUMO) for closed-shell chemical species.[9]

In 1987, on the basis of considerable circumstantial evidences, Pearson concluded that "there seems to be a rule of nature that molecules arrange themselves so as to be as hard as possible",[10] which is known as the principle of maximum hardness (PMH). In 1991, Parr et al. have given a rigorous and widely general proof of the PMH.[11−13] The PMH asserts that chemical systems arrange themselves so as to be as hard as possible under the constraints where μ and v both remain constant. The PMH has been verified by examining the variation of η along vibrational symmetry coordinates of the molecules.[14−18]

In 1992, based on the obseravations made from the numerical results, Datta introduced one interesting corollary of the PMH.[15] According to his corollary, the transition state (TS) of a chemical reaction is likely to have a minimum value of η along the reaction coordinate, since the value of η tends to decrease upon a chemical species moving away from its equilibrium position.[11] Since then, the variation of η along a reaction coordinate, i.e. η profile, has been discussed in the light of the PMH. There have been reported a large number of papers regarding η profiles of various types of chemical reactions, such as isomerization reactions,[19−23] intermolecular-[24,25] and intramolecular-proton-transfer reactions,[15,26] cycloaddition reactions,[27−30] intramolecular rearrangement reactions,[31] and van der Waals complexes.[32] Moreover, η profiles for internal bond rotation have also been extensively examined.[18,20,21,33−39] In these papers, it has been commonly shown that a more stable structure along the reaction coordinate is associated with a higher value of η and a lower value of μ. The computed η profiles usually go through a minimum in the TS regions, although, in some cases, the position of η maximum is significantly deviated from that of the TS.[22,23,27,28,30,40] Only in very exceptional cases, η profiles do not yield an extremum along the reaction coordinate.[29,32]

These results appear to support Datta's corollary in most of the cases. Namely, although neither μ nor v remains constant along a reaction coordinate in general, it would seem that the PMH holds for the variation of η along the reaction coordinate. However, the above-mentioned η profile investigations have been limited to those for closed-shell chemical species. Meanwhile, investigations on η profiles for open-shell chemical species are very few. Recently, Sannigrahi et al. have extended η profile investigation to open-shell species.[41] They found that η profiles for isomerization reactions of the $^1A'$ state of HNO−

* Corresponding author. Tel. +81-298-61-4522. Fax: +81-298-61-4487. E-mail: t_uchimaru@home.nimc.go.jp.

10.1021/jp003257s CCC: $20.00 © 2001 American Chemical Society
Published on Web 02/02/2001

HON and of the $^2A''$ state of HSO−HOS show the salient features expected from the corollary of the PMH. Nevertheless, the $^3A''$ state of HNO−HON isomerization was found to be associated with a quite erratic η profile.

In the present study, we have focused our attention upon internal bond rotation in substituted methyl radicals, X-CH_2 (X = BH_2, CH_3, NH_2, and OH). We examined the rotational energy profiles of these radicals by using B3LYP[42] and QCISD(T)[43] calculations. The computed rotational energy profiles, as well as the calculated values for the geometrical parameters, the vibrational frequencies and the ionization potential, were in reasonable agreement with previously reported experimental and theoretical results. In addition, we examined the variation of μ and η along the rotational coordinates of the radicals. We describe herein that the features of the profiles of μ and η for internal bond rotation of the open-shell doublet-state of these radicals are quite different from those expected from the corollary of the PMH. In particular, the profiles of μ and η for internal bond rotation of H_2N-CH_2 and $HO-CH_2$ radicals present striking contrast to those reported for internal bond rotation of closed-shell chemical species.

2. Computational Details

In general, an unrestricted Hartree−Fock (UHF) wave function is spin-contaminated for open-shell chemical species. Moreover, Koopmans' approximation cannot be unambiguously applied to an UHF wave function.[41] Thus, it is somewhat difficult to evaluate reasonable values of μ and η on the basis of the orbital energies of the radicals.

Spin contamination in an UHF wave function is carried forward to conventional post-HF calculations, i.e., Moller−Plesset perturbation methods. It has been shown that QCISD method is much less affected by spin contamination among post-HF methods.[44,45] Meanwhile, the approximate functionals currently used in density functional theory (DFT) computations appear to have much less spin contamination than UHF calculations,[46] even for a TS.[47] In particular, B3LYP method is known to be quite reliable to study of electronic structure and energetics of various chemical species, including open-shell chemical species.[41,48,49] Moreover, recent computational investigations show that B3LYP calculations describe quite well the behavior of internal bond rotation of open-shell chemical species.[50,51]

Thus, we examined the rotational energy profiles of the substituted methyl radicals by using B3LYP[42] and QCISD(T)[43] calculations. The values of μ and η were calculated according to three-point approximation, namely eqs 2a and 2b. The values of IP and EA were computed by performing separate calculations for the neutral radical and its cationic and anionic counterparts at the geometry of the neutral system (ΔSCF procedure). This procedure has been successfully applied for the evaluation of the values of μ and η for open-shell chemical species.[41,52−54] Due to the admixture of HF exchange, B3LYP method usually has somewhat higher spin contamination as compared with pure DFT methods.[46] But we did not use spin projection procedure, not only because Schlegel et al. reported that spin projection can seriously degrade the quality of potential energy surface calculated with DFT methods,[46] but also because spin contamination in our B3LYP calculations was insignificant: the value of S^2 ranged from 0.752 to 0.755.

Geometry optimizations of the radicals were carried out by using B3LYP method in conjunction with 6-31G(d) basis set [B3LYP/6-31G(d)]. The geometrical parameters were optimized for each value of dihedral angle θ about the X−C bond, whose

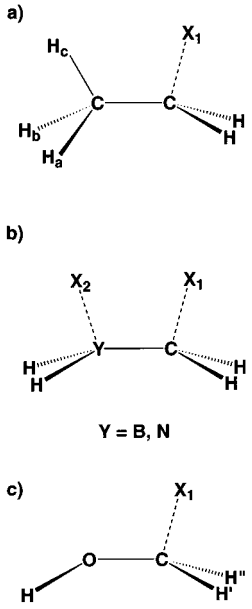

Figure 1. The definition of geometrical parameters of the radicals. Point X_1 is placed on the line going through carbon atom, which is perpendicular to the H−C−H plane. Similarly, the point X_2 is placed on the line going through atom Y, which is perpendicular to the H−Y−H plane. The angle θ is defined as follows: dihedral angle of $X_1-C-Y-X_2$ for H_2B-CH_2 and H_2N-CH_2 radicals, dihedral angle of $X_1-C-C-H_a$ for H_3C-CH_2 radical, and dihedral angle of $X_1-C-O-H$ for $HO-CH_2$ radical.

definitions are given in Figure 1. The stationary points along the rotational coordinates were fully optimized and then vibrational frequency calculations were carried out at the optimized geometries. The energy of each optimized structure was evaluated with single-point calculations of B3LYP and QCISD(T) methods using a larger basis set, 6-311+G(2df,2p), i.e., B3LYP/6-311+G(2df,2p) and QCISD(T)/6-311+G(2df,-2p). The values of IP and EA were also calculated at these computational levels. Hereafter we refer to the computational levels of B3LYP/6-31G(d)//B3LYP/6-31G(d), B3LYP/6-311+G-(2df,2p)//B3LYP/6-31G(d), and QCISD(T)/6-311+G(2df,2p)//B3LYP/6-31G(d) merely as B3LYP-1, B3LYP-2, and QCISD-(T), respectively. Table 1 gives the total energies and the zero-point vibrational energies for the stationary points along the rotational coordinates of the radicals. The program suite of GAUSSIAN 98[55] was employed for all the calculations.

3. Results

3.1 Geometries. Table 2 shows the B3LYP-1 optimized geometrical parameters for the equilibrium and the rotational TS structures of the radicals. The optimized structures are illustrated in Figure 2. The geometrical features of the rotational stationary points of the radicals are in good agreement with those reported in precedent *ab inito* works. Moreover, the computed rotational energy profiles are in accord with previously reported ones.

For the H_2B-CH_2 radical, the equilibrium and the rotational TS structures both have C_{2v} symmetry. The H−B−H and H−C−H planes are coplanar in the equilibrium structure (θ = 0.0°), while these planes are perpendicular to each other in the TS (θ = 90.0°). For H_3C-CH_2 radical, the equilibrium (θ = 60.7°) and the rotational TS (θ = 90.0°) structures both have C_s symmetry. In the TS, the radical center of CH_2 moiety is planar and lies on the symmetry plane, while the radical center is slightly pyramidalized in the equilibrium structure: the angle

TABLE 1: Total Energies (au) and Zero-Point Vibrational Energies (kcal/mol) of the Radicals and Related Charged Species

	symmetry	B3LYP-1[a]	ZPE[b]	B3LYP-2[c]	QCISD(T)[d]
H_2B-CH_2 (Eq.)	C_{2v}	−65.28893	27.30	−65.31324	−65.13073
H_2B-CH_2 (Eq.)[e]	C_{2v}			−64.92193	−64.74797
$H_2B-CH_2^-$ (Eq.)[e]	C_{2v}			−65.37844	−65.19446
H_2B-CH_2 (TS)	C_{2v}	−65.27359	25.68	−65.29973	−65.11633
$H_2B-CH_2^+$ (TS)[e]	C_{2v}			−64.98050	−64.79720
$H_2B-CH_2^-$ (TS)[e]	C_{2v}			−65.29327	−65.10460
$HB-CH_3^+$[f]	C_{3v}	−65.01698	28.65	−65.03865	−64.86135
H_3C-CH_2 (Eq.)	C_s	−79.15787	37.44	−79.18997	−78.99285
H_3C-CH_2+ (Eq.)[e]	C_s			−78.87469	−78.67984
$H_3C-CH_2^-$ (Eq.)[e]	Cs			−79.17231	−78.96900
H_3C-CH_2 (TS)	C_s	−79.15773	37.24	−79.18989	−78.99271
H_3C-CH_2 (TS)[e]	C_s			−78.87570	−78.68083
$H_3C-CH_2^-$ (TS)[e]	C_s			−79.17187	−78.96842
$C_2H_5^+$[g]	C_{2v}	−78.86011	38.29	−78.88894	−78.69742
H_2N-CH_2 (Eq.)	C_s	−95.19561	31.70	−95.24302	−95.03107
$H_2N-CH_2^+$ (Eq.)[e]	C_s			−94.97166	−94.77169
$H_2N-CH_2^-$ (Eq.)[e]	C_s			−95.20002	−94.98271
H_2N-CH_2 (TS)	C_s	−95.18020	30.15	−95.22694	−95.01648
$H_2N-CH_2^+$ (TS)[e]	C_s			−94.89432	−94.68821
$H_2N-CH_2^-$ (TS)[e]	C_s			−95.21187	−94.99467
$H_2N-CH_2^+$	C_s	−94.97410	34.17	−95.01138	−94.80882
$HO-CH_2$ (Eq.)	C_s	−115.05203	23.54	−115.10904	−114.88034
$HO-CH_2^+$ (Eq.)[e]	C_s			−114.80154	−114.58408
$HO-CH_2^-$ (Eq.)[e]	C_s			−115.07619	−114.84037
$HO-CH_2$ (TS−1)	C_s	−115.04437	22.30	−115.10148	−114.87285
$HO-CH_2^+$ (TS−1)[e]	C_s			−114.76773	−114.54643
$HO-CH_2^-$ (TS−1)[e]	C_s			−115.08313	−114.84785
$HO-CH_2$ (TS−2)	C_s	−115.05098	22.66	−115.10896	−114.87994
$HO-CH_2^+$ (TS−2)[e]	C_s			−114.81424	−114.59664
$HO-CH_2^-$ (TS−2)[e]	C_s			−115.07046	−114.83363
$HO-CH_2^+$	C_s	−114.78250	25.52	−114.82949	−114.61003

[a] B3LYP/6-31G(d)//B3LYP/6-31G(d). [b] Zero-point vibrational energy calculated at B3LYP-1 level (not scaled). [c] B3LYP/6-311+G(2df,2p)//B3LYP/6-31G(d). [d] QCISD(T)/6-311+G(2df,2p)//B3LYP/6-31G(d). [e] Charged species with the geometry of the stationary point of neutral species given in the parenthesis. [f] The global minimum structure of CH_4B^+ species with C_{3v} symmetry ($HB-CH_3^+$) (ref 84). [g] The global minimum structure of $C_2H_5^+$ species with C_{2v} symmetry (bridged structure) (ref 57).

$C-C-X_1$ is 98.4°. The differences between B3LYP-1 optimized bond lengths and the corresponding values optimized with post-HF methods, such as MP2[45,56−58] and QCISD[45] calculations, are less than 0.01 Å. The differences for the bond angles are less than 0.5°.

The C_s symmtery is also found in the equilibrium ($\theta = 0.0°$) and the TS ($\theta = 90.0°$) structures for the H_2N-CH_2 radical. The nitrogen atom is pyramidalized in both the structures: the angle $C-N-X_2$ is 45.3 and 35.8°, respectively, in the equilibrium and the TS structures. The CH_2 moiety is planar and lies on the symmetry plane in the TS, while the equilibrium structure has the pyramidalized radical center ($N-C-X_1 = 123.9°$). The B3LYP-1 optimized geometrical parameters for the equilibrium structure are very close to the MP2 optimized values.[59]

The equilibrium structure of the $HO-CH_2$ radical is totally nonsymmetric ($\theta = 79.7°$). Meanwhile, the two C_s structures found along the rotational coordinate both correspond to TS's, TS-1 ($\theta = 0.0°$) and TS-2 ($\theta = 90.0°$). The CH_2 moiety is planar in TS-2, whereas the equilibrium and TS-1 structures have a pyramidalized CH_2 moiety: angle $O-C-X_1$ is 120.8 and 112.5°, respectively. The B3LYP-1 optimized geometrical parameters are comparable to the corresponding MP2 values.[59−64] The differences between B3LYP-1 and the MP2 values are less than 0.01 Å and 1°, respectively, for the bond lengths and the bond angles in most of the cases.

3.2. Vibrational Frequencies. The vibrational frequencies calculated at B3LYP-1 level are given in Table 3. The frequencies are scaled using a factor of 0.9614, which has been prescribed for B3LYP-1 frequencies.[65] To the best of our knowledge, experimentally observed frequencies have been reported only for the CH_3-CH_2 and $HO-CH_2$ radicals (see Table 3). The calculated frequencies reproduce the experimentally observed values moderately well. But the assignment of infrared peak at 569 cm^{-1} for the $HO-CH_2$ radical is still controversial. Although the MP2 calculations by Bauschlicher et al. supported the existence of this peak,[66] Johnson et al. concluded that this peak should not belong to the $HO-CH_2$ radical.[61,62]

It may be worthwhile to discuss the change in the harmonic vibrational frequencies while going from the equilibrium states to the TSs. The stretching vibrational modes are generally not contaminated with other modes of vibrations. The frequencies associated with stretching modes in the equilibrium structures and in the TSs can be relatively easily compared with each other. For the H_2B-CH_2 radical, the symmetric and the antisymmetric C−H stretching frequencies remain almost unchanged on going from the equilibrium (3014 and 3087 cm^{-1}) to the TS (3020 and 3090 cm^{-1}), whereas the B−H stretching frequencies change significantly, from 2513 and 2583 cm^{-1} in the equilibrium to 2458 and 2504 cm^{-1} in the TS. Similarly, for the H_2N-CH_2 radical, the changes in the C−H stretching frequencies are less significant as compared with those of the N−H stretching frequencies: on going from the equilibrium to the TS, the frequencies of the C−H stretching vary from 3028 and 3129 cm^{-1} to 2978 and 3098 cm^{-1}, whereas the N−H frequencies vary from 3373 and 3469 cm^{-1} to 3282 and 3340 cm^{-1}. For the H_3C-CH_2 radical, the C−H stretching frequencies of CH_2 group (3047 and 3139 cm^{-1}), as well as those of CH_3 group (2852, 2941, and 2983^{-1}), in the equilibrium structure remain almost unchanged in the TS. Quite noteworthy is the changes in the O−H and C−H stretching frequencies for the $HO-CH_2$

TABLE 2: Geometrical Parameters Optimized at B3LYP/6-31G(d) Level[a]

		H_2B-CH_2			
		Eq. (C_{2v})			
B−C	1.532	H−B−C	120.3	H−B−H	119.4
B−H	1.197	H−C−B	123.3	H−C−H	113.5
C−H	1.090	B−C−X_1	90.0	C−B-X_2	90.0
		X_1-C-B−X_2	0.0		
		TS (C_{2v})			
B−C	1.530	H−B−C	122.0	H−B−H	116.0
B−H	1.205	H−C−B	122.9	H−C−H	114.2
C−H	1.090	B−C−X_1	90.0	C−B-X_2	90.0
		X_1-C-B−X_2	90.0		
		H_3C-CH_2			
		Eq. (C_s)			
C−C	1.490	H_a-C−C	111.8	H_b−C−C	112.1
C−H_a	1.097	H_c-C−C	111.8	C−C−H′	120.9
C−H_b	1.105	C−C−H″	120.9	C−C−X_1	98.4
C−H_c	1.097	H_a-C-C−X_1	60.7		
C−H′	1.085				
C−H″	1.085				
		TS (C_s)			
C−C	1.490	H_a-C−C	111.9	H_b-C−C	111.9
C−H_a	1.095	H_c-C−C	111.9	C−C−H′	121.8
C−H_b	1.102	C−C−H″	120.6	C−C−X_1	90.0
C−H_c	1.102	H_a-C-C−X_1	90.0		
C−H′	1.084				
C−H″	1.086				
		H_2N-CH_2			
		Eq. (C_s)			
N−C	1.402	H_a-N−C	114.1	H_b−N−C	114.1
N−H_a	1.015	H_a-N−H_b	109.8	N−C−H′	115.6
N−H_b	1.015	N−C−H″	115.6	H′−C−H″	117.3
C−H′	1.086	C−N−X_2	45.3	N−C−X_1	123.9
C−H″	1.086	X_1-C-N−X_2	0.0		
		TS (C_s)			
N−C	1.422	H_a−N−C	110.8	H_b-N−C	110.8
N−H_a	1.022	H_a−N−H_b	105.3	N−C−H′	123.0
N−H_b	1.022	N−C−H″	118.3	H′−C−H″	118.7
C−H′	1.092	C−N−X_2	35.8	N−C−X_1	90.0
C−H″	1.086	X_1-C−N−X_2	90.0		
		HO−CH_2			
		Eq. (C_1)			
O−C	1.370	H−O−C	108.9	O−C−H′	118.5
O−H	0.969	O−C−H″	112.6	H′−C−H″	119.7
C−H′	1.089	O−C−X_1	120.8	H−O−C−X_1	79.7
C−H″	1.084				
		TS-1 (C_s)			
O−C	1.372	H−O−C	110.4	O−C−H′	117.4
O−H	0.971	O−C−H″	117.4	H′−C−H″	120.2
C−H′	1.089	O−C−X_1	112.5	H−O−C−X_1	0.0
C−H″	1.089				
		TS-2 (C_s)			
O−C	1.368	H−O−C	109.0	O−C−H′	121.0
O−H	0.968	O−C−H″	114.9	H′−C−H″	124.1
C−H′	1.082	O−C−X_1	90.0	H−O−C−X_1	90.0
C−H″	1.079				

[a] Bond lengths are given in angstroms, whereas bond angles and dihedral angles are given in degrees.

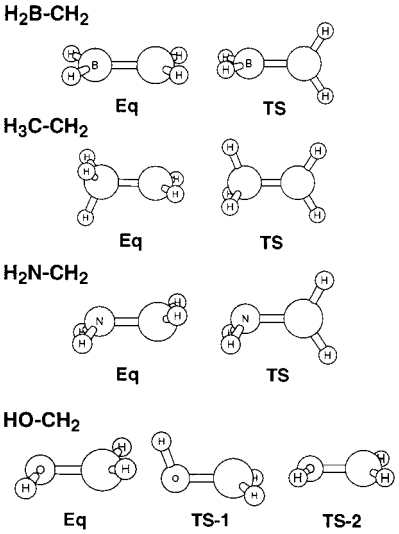

Figure 2. The graphical views of the rotational stationary points of the radicals.

TABLE 3: Vibrational Frequencies of the Radicals

	H_2B-CH_2			H_3C-CH_2		
	Eq. (calcd)[a]	TS (calcd)[a]		Eq. calcd[a]	Eq. obsd[b]	TS (calcd)[a]
ν_1	128	766*i*	ν_1	117		127*i*
ν_2	641	343	ν_2	440	540	419
ν_3	742	516	ν_3	786		789
ν_4	945	775	ν_4	956		950
ν_5	1015	974	ν_5	1033	1175	1032
ν_6	1024	1039	ν_6	1161	1138	1159
ν_7	1224	1193	ν_7	1375		1376
ν_8	1442	1357	ν_8	1435	1366	1437
ν_9	2513	2458	ν_9	1452	1440	1445
ν_{10}	2583	2504	ν_{10}	1456	1440	1462
ν_{11}	3014	3020	ν_{11}	2852	2842	2878
ν_{12}	3087	3090	ν_{12}	2941	2920	2905
			ν_{13}	2983	2987	2994
			ν_{14}	3047	3033	3050
			ν_{15}	3139	3112	3145

	H_2N-CH_2			HO−CH_2			
	Eq. (calcd)[a]	TS (calcd)[a]		Eq. calc.[a]	Eq. obsd.[c]	TS-1 (calcd)[a]	TS-2 (calcd)[a]
ν_1	439	585*i*	ν_1	433	420	568*i*	496*i*
ν_2	662	388	ν_2	654	[569][d]	502	370
ν_3	763	810	ν_3	1031	1048	1069	1009
ν_4	921	1062	ν_4	1172	1183	1121	1179
ν_5	1179	1105	ν_5	1328	1334	1203	1323
ν_6	1295	1141	ν_6	1449	1459	1465	1448
ν_7	1440	1465	ν_7	3006	[2915]	2991	3071
ν_8	1622	1609	ν_8	3145	[3019]	3103	3211
ν_9	3028	2978	ν_9	3616	3650	3546	3628
ν_{10}	3129	3098					
ν_{11}	3373	3282					
ν_{12}	3469	3340					

[a] The calculated frequencies are scaled by a factor of 0.9614 (ref 65) except for imaginary frequencies. [b] Reference 85. [c] Referencess 86 and 87. [d] See ref 61.

radical. In TS-1, the O−H stretching frequency of 3546 cm^{-1} is lower by 70 cm^{-1} than that (3616 cm^{-1}) in the equilibrium structure and the C−H stretching frequencies of 2991 and 3103 cm^{-1} are also lower as compared with those of 3006 and 3145 cm^{-1} in the equilibrium structure. The opposite changes are observed for TS-2. The C−H stretching frequencies of 3071 and 3211 cm^{-1} in TS-2 are significantly higher than those in the equilibrium structure and the O−H stretching frequency is also slightly higher in TS-2 (3628 cm^{-1}) than that in the equilibrium structure.

Apart from bond stretching, the vibrational modes are generally coupled with each other and the coupling patterns are

TABLE 4: Rotational Barrier Heights (in kcal/mol) for Internal Rotation of the Radicals[a]

		B3LYP-1[b]	B3LYP-2[c]	QCISD(T)[d]	exptl.
H_2B-CH_2		9.63	8.48	9.04	
		(8.04)	(6.89)	(7.45)	
H_3C-CH_2		0.09	0.05	0.09	
		(−0.11)	(−0.15)	(−0.11)	0.06[e]
H_2N-CH_2		9.67	10.09	9.16	
		(8.15)	(8.57)	(7.64)	
$HO-CH_2$	TS-1	4.81	4.74	4.70	
		(3.59)	(3.53)	(3.48)	4.6[f]
	TS-2	0.66	0.05	0.25	
		(−0.20)	(−0.81)	(−0.61)	

[a] Values in the parentheses include zero-point energy corrections, which are scaled by a factor of 0.9806 (ref 65). [b] B3LYP/6-31G(d)// B3LYP/6-31G(d) [c] B3LYP/6-311+G(2df,2p)// B3LYP/6-31G(d) [d] QCISD(T)/6-311+G(2df,2p)// B3LYP/6-31G(d) [e] Reference 72. [f] Reference 73.

significantly altered on going from the equilibrium to the TS. Thus, except for the stretching modes, we cannot always find out one to one correspondence between the normal modes for the equilibrium and the TS. But the bending modes of the CH_2 and BH_2 groups in the H_2B-CH_2 radical and those of the CH_2 and NH_2 groups in the H_2N-CH_2 radical can be clearly distinguished from other modes. For the H_2B-CH_2 radical, the frequencies of CH_2 and BH_2 bending modes in the equilibrium are 1442 and 1224 cm^{-1}, respectively. The corresponding frequencies in the TS are 1357 and 1193 cm^{-1}. For the H_2N-CH_2 radical, the frequencies of the CH_2 and NH_2 bending modes in the equilibrium are 1440 and 1622 cm^{-1}, respectively. The corresponding frequencies in the TS are 1465 and 1609 cm^{-1}. It might be noteworthy that the frequency of CH_2 bending mode in H_2B-CH_2 radical significantly decreases by 85 cm^{-1} on going from the equilibrium to the TS.

3.3. Rotational Barrier Heights. Table 4 gives the calculated values, as well as the experimentally measured values, for the barrier heights of the internal bond rotation in the radicals (see also Figures 3−6). The zero-point vibrational energies are scaled by a factor of 0.9806.[65] The B3LYP-1, B3LYP-2, and QCISD-

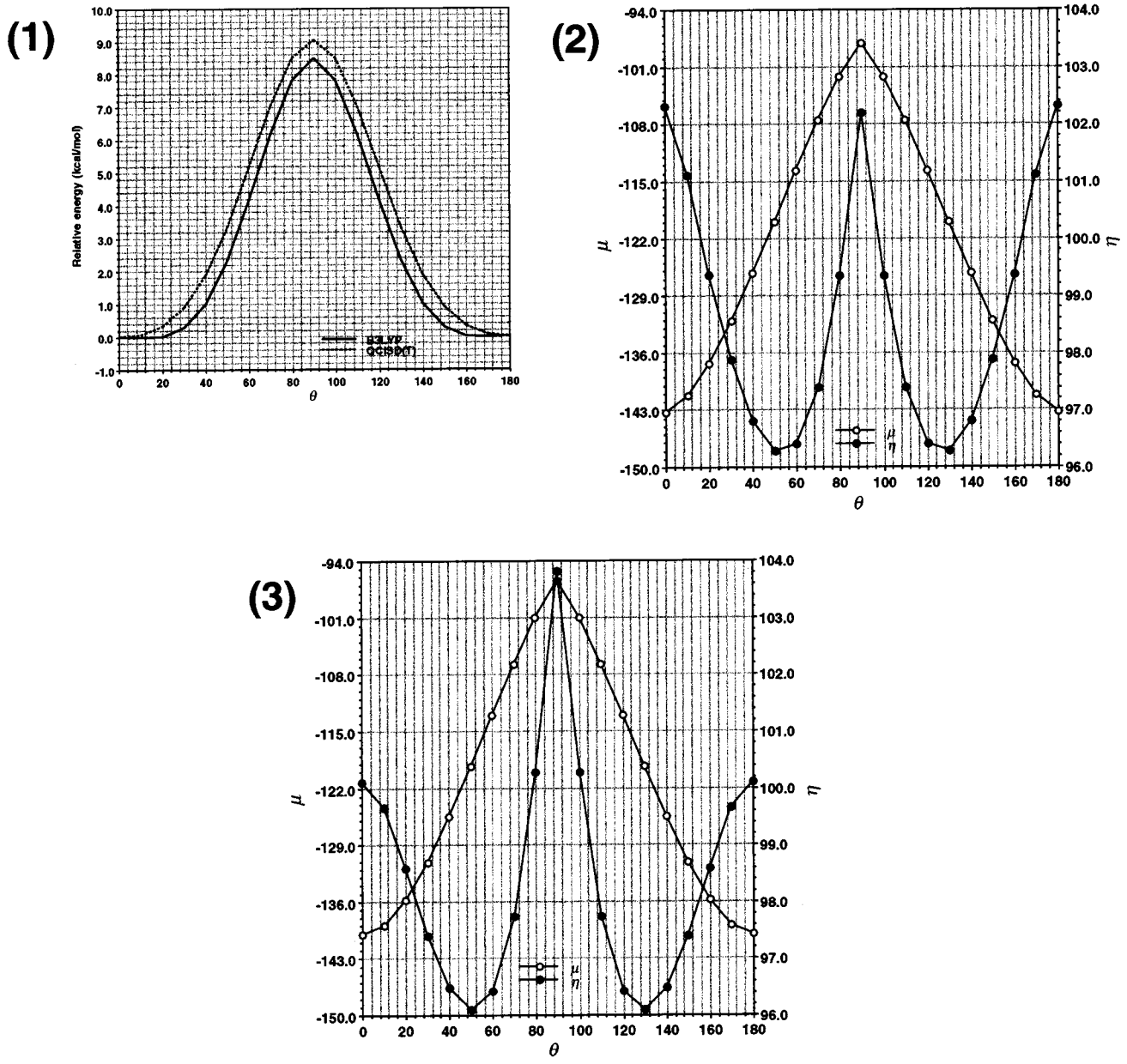

Figure 3. The rotational profiles for H_2B-CH_2 radical; the rotational potential energy profile (1); the rotational μ (open circles) and η (closed circles) profiles computed at B3LYP-2 level (2); the rotational μ (open circles) and η (closed circles) profiles computed at QCISD(T) level (3).

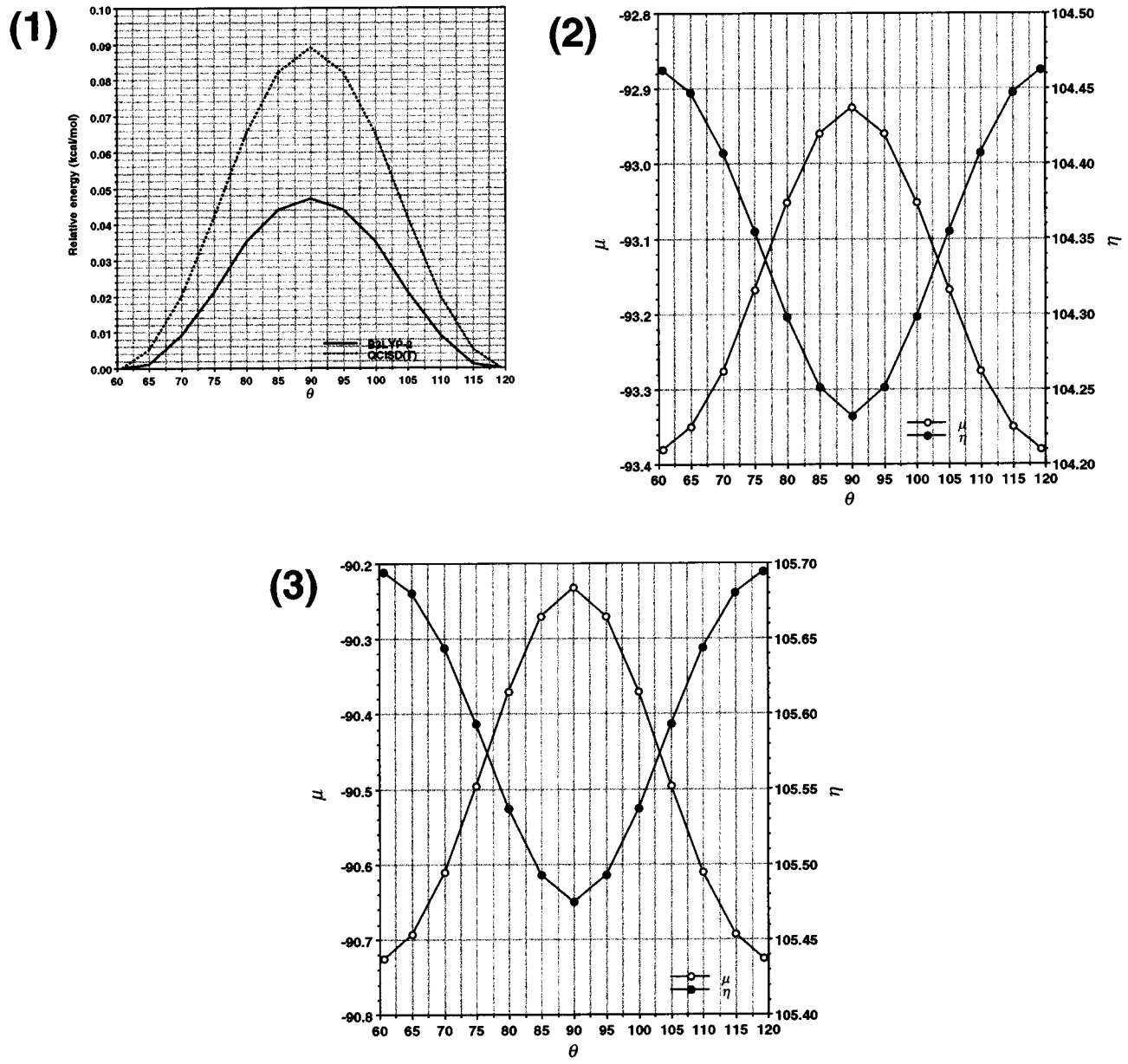

Figure 4. The rotational profiles for H_3C-CH_2 radical; the rotational potential energy profile (1); the rotational μ (open circles) and η (closed circles) profiles computed at B3LYP-2 level (2); the rotational μ (open circles) and η (closed circles) profiles computed at QCISD(T) level (3).

(T) values for the rotational barrier of H_2B-CH_2 radical range from 8 to 9 kcal/mol, which is consistent with the MP4/6-31G-(d) results reported by Borden et al.: their results indicate that the energy difference between the equilibrium structure and the 90° twisted structure about the B−C bond is 9.7 kcal/mol.[66]

The rotational barrier for H_3C-CH_2 radical is very small. Our estimates are less than the order of 0.1 kcal/mol and after zero-point vibrational energy correction, the values for the barrier height become slightly negative. The previously reported ab initio rotational barrier heights for the H_3C-CH_2 radical are comparable to ours.[56,67−69] The most recently reported theoretical value for the barrier height of H_3C-CH_2 radical is 26 cm^{-1} (0.07 kcal/mol).[70] These results suggest that the torsional motion in the H_3C-CH_2 radical undergoes free internal rotation, which is consistent with the experimental observation[71] and also with the experimentally derived value of 20 cm^{-1} (0.06 kcal/mol) for the rotational barrier.[72]

The rotational barrier of H_2N-CH_2 radical is the largest among the radicals studied in the present work. The B3LYP-1, B3LYP-2, and QCISD(T) barrier heights range from 9 to 10 kcal/mol, which is comparable to the MP4/6-31G(d) results reported by Borden et al., indicating the difference in energy of 8.5 kcal/mol between the equilibrium structure of H_2N-CH_2 radical and the 90° twisted structure about N−C bond.[66] Zero-point vibrational energy correction leads to the rotational energy barrier around 8 kcal/mol, which is very close to the MP4 value of 8.37 kcal/mol reported by Peeters et al.[69]

For $HO-CH_2$ radical, the B3LYP-1, B3LYP-2, and QCISD-(T) barrier heights for TS-1 range from 4.7 to 4.8 kcal/mol. These values are very close to the MP2 values reported by Bruna et al.[61] and by Johnson et al.[62] Our estimates around 3.5 kcal/mol including zero-point vibrational energy correction are slightly smaller than the experimentally derived value of 4.6 kcal/mol reported by Krusic et al.[73] After adding the correction for level of correlation treatment and for basis set improvement, Bauschlier et al.[74] reported a theoretical estimate of 4.7 kcal/mol for the barrier height of $HO-CH_2$ radical, which is very close to the experimental value.[73] Meanwhile, the barrier height for TS-2 is very small. Our estimates of the barrier height for TS-2 are less than 1 kcal/mol and zero-point vibrational energy

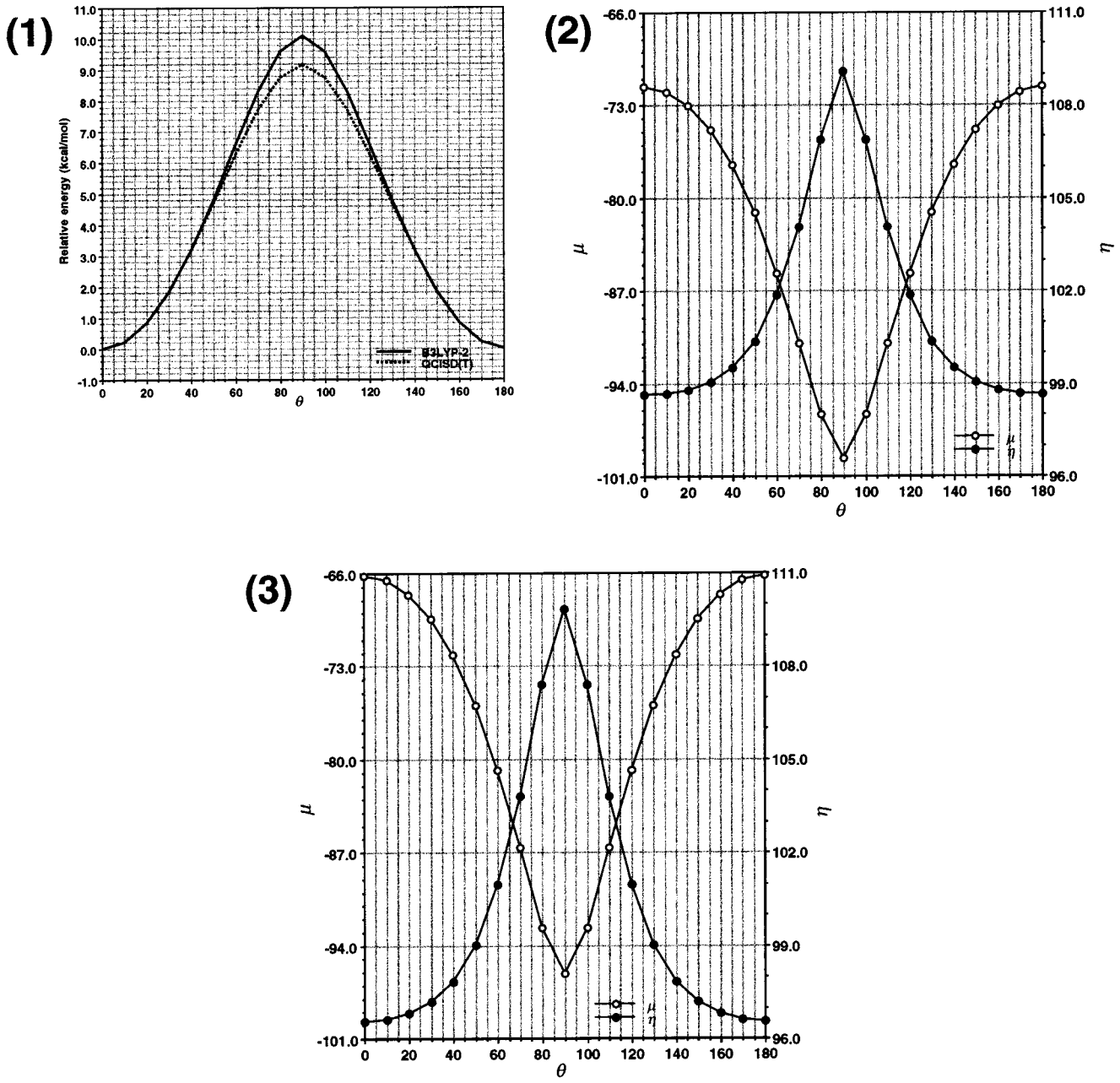

Figure 5. The rotational profiles for H_2N-CH_2 radical; the rotational potential energy profile (1); the rotational μ (open circles) and η (closed circles) profiles computed at B3LYP-2 level (2); the rotational μ (open circles) and η (closed circles) profiles computed at QCISD(T) level (3).

correction leads to slightly negative values. The previously reported MP2 results[61,62] are comparable to ours.

3.4. Ionization Potentials. For the H_3C-CH_2, H_2N-CH_2, and $HO-CH_2$ radicals, the experimentally measured values for IP have been reported. Thus, we compared the calculated IP values with the experimental values (see Table 5). The values of IP calculated with B3LYP-2 level are larger by 0.06−0.32 eV than those calculated with QCISD(T) level. The estimates derived from our QCISD(T) level calculations are in moderate agreement with the experimentally measured vertical, as well as adiabatic, IP's. Brinck et al.[75] computed the values for adiabatic IP using the G2MS[76] procedure: their values are very close to our QCISD(T) values.

3.5. Variation of μ and η along the Rotational Coordinates. The values of μ and η at the stationary points along the rotational coordinates are given in Table 6. Figures 3−6 show rotational potential energy profiles as well as the corresponding μ and η profiles. Although the QCISD(T) values for μ and η are less negative/larger than the corresponding B3LYP-2 values in most of the cases, the differences between the B3LYP-2 and the QCISD(T) profiles of μ and η, as well as those of potential energies are not pronounced.[77]

For the H_2B-CH_2 radical, the maximum value of μ is associated with the rotational TS ($\theta = 90.0°$). The value of μ gradually decreases on going away from the TS and reaches the minimum value at the equilibrium structure ($\theta = 0.0$ and 180.0°) (see Figure 3). Meanwhile, the minimum value of η appears in the structure with θ being around 50 or 130°, which corresponds to neither the equilibrium nor the TS structure. While the B3LYP-2 η values for the equilibrium and the TS structures are comparable to each other, 102.32 and 102.19 kcal/mol, respectively (see Table 6), the QCISD(T) η value is larger (103.81 kcal/mol) in the TS than in the equilibrium structure (100.10 kcal/mol). The rotational TS for the H_2B-CH_2 radical corresponds to the maximum, at least the local maximum, value of η.

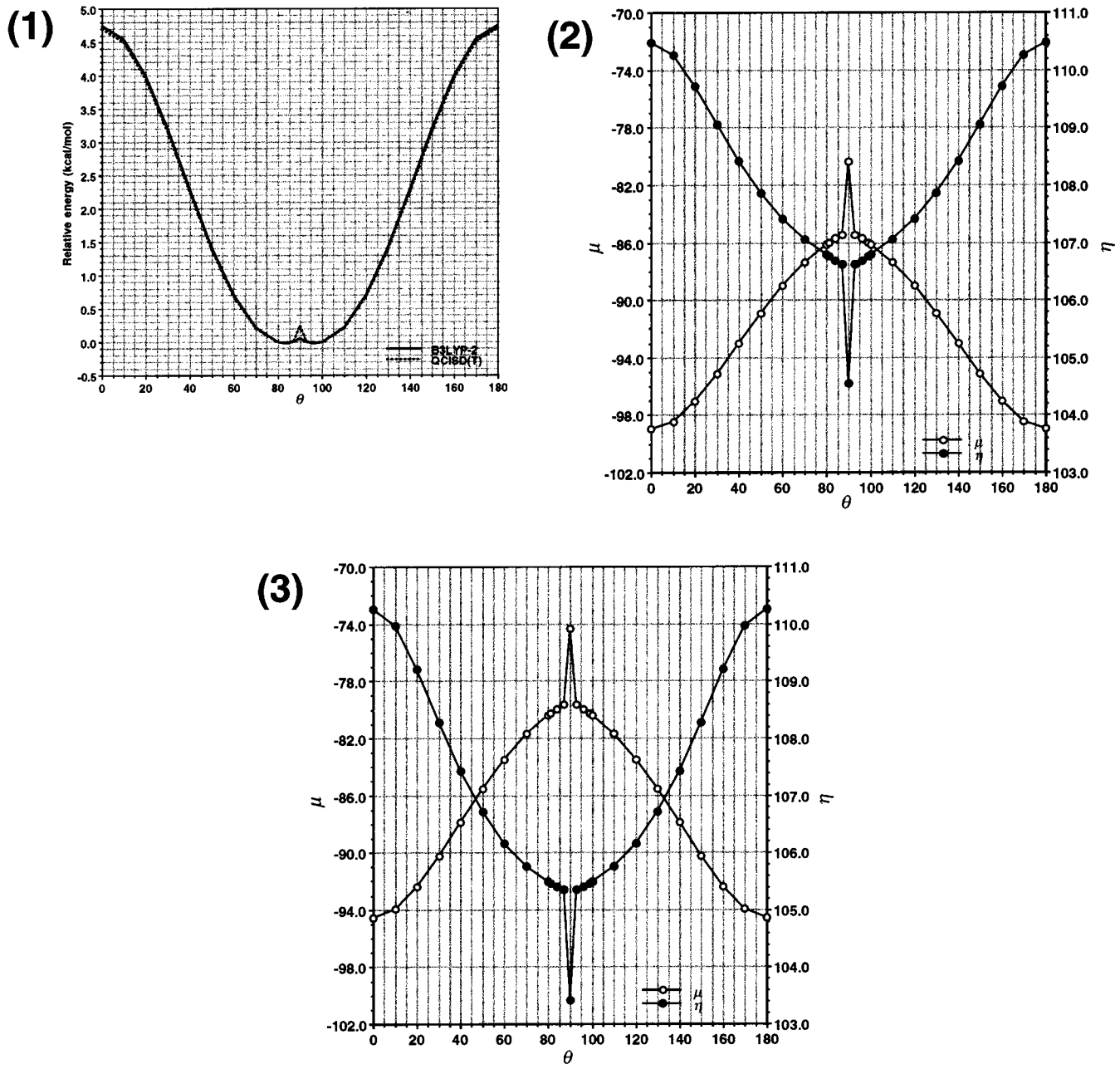

Figure 6. The rotational profiles for $HO-CH_2$ radical; the rotational potential energy profile (1); the rotational μ (open circles) and η (closed circles) profiles computed at B3LYP-2 level (2); the rotational μ (open circles) and η (closed circles) profiles computed at QCISD(T) level (3).

TABLE 5: Ionization Potentials (eV) of the Radicals

	vertical			adiabatic			
	calcd			calcd			
	B3LYP-2[a]	QCISD(T)[b]	exptl	B3LYP-2[a]	QCISD(T)[b]	G2MS[c]	exptl
H_2B-CH_2	10.65	10.42		7.53	7.39		
H_3C-CH2	8.58	8.52		8.23	8.08	8.05	8.117 ± 0.008[d] 8.26 ± 0.02[e] 8.39 ± 0.02[f]
H_2N-CH_2	7.38	7.06	6.97 ± 0.03[g]	6.41	6.15	6.13	6.3[h] 6.29 ± 0.03[g]
$HO-CH_2$	8.37	8.06	8.14 ± 0.01[i]	7.69	7.44	7.43	7.553 ± 0.006[d,j] 7.56 ± 0.02[k] 7.56 ± 0.01[i]

[a] B3LYP/6-311+G(2df,2p)//B3LYP/6-31G(d). [b] QCISD(T)/6-311+G(2df,2p)//B3LYP/6-31G(d). [c] Reference 75. [d] References 57 and 88. [e] Reference 89. [f] Reference 90. [g] Reference 91. [h] Reference 92. [i] Reference 93. [j] Reference 94. [k] Reference 95.

For the H_3C-CH_2 radical, the value of η and the potential energy behave in an opposite fashion: the maximum and the minimum values of η are associated with the equilibrium and the TS structures, respectively (see Figure 4). Interestingly, for

TABLE 6: Calculated Values for Chemical Potential (μ), Hardness (η), and Polarizability (α)

		chemical potential (μ)[a]		hardness (η)[a]		polarizability (α)[b]	
		B3LYP-2[c]	QCISD(T)[d]	B3LYP-2[c]	QCISD(T)[d]	B3LYP-2[c]	QCISD(T)[d]
H_2B-CH_2	Eq.	−143.23	−140.09	102.32	100.10	28.541	27.565
	$\theta = 50$	−120.04	−119.39	96.28	96.09	29.442	27.974
	TS	−98.13	−96.45	102.19	103.81	28.465	27.014
H_3C-CH_2	Eq.	−93.38	−90.73	104.46	105.69	26.904	25.778
	TS	−92.93	−90.23	104.23	105.48	26.871	25.741
H_2N-CH_2	Eq.	−71.65	−66.21	98.63	96.56	25.313	24.443
	TS	−99.63	−96.15	109.09	109.84	23.319	22.413
$HO-CH_2$	Eq.	−86.17	−80.41	106.79	105.49	19.627	18.857
	TS-1	−98.96	−94.57	110.47	110.26	18.961	18.252
	TS-2	−80.39	−74.36	104.55	103.42	19.573	18.812

[a] In kcal/mol. [b] In au. [c] B3LYP/6-311+G(2df,2p)//B3LYP/6-31G(d). [d] QCISD(T)/6-311+G(2df,2p)//B3LYP/6-31G(d).

the H_2N-CH_2 radical, the value of η behaves in a fashion completely opposite from that observed for H_3C-CH_2 radical (see Figure 5). The maximum and the minimum values of η appear in the TS and the equilibrium structures, respectively. For the $HO-CH_2$ radical, the maximum and the minimum values of η appear in TS-1 ($\theta = 0.0$ and 180°) and TS-2 ($\theta = 90.0°$), respectively, and the equilibrium structure does not correspond to the extremum of η (see Figure 6). It is observed commonly for the H_3C-CH_2, H_2N-CH_2, and $OH-CH_2$ radicals that the behavior of μ is opposite to those of η: the maximum and the minimum values of η are associated with the minimum and the maximum values of μ, respectively. Such opposite behavior of μ and η along a reaction coordinate was frequently observed for closed-shell chemical species.[20−22,26,36]

In our recent paper,[78] we discussed the conditions in which μ or η goes through an extremum. We have shown that both μ and η always go through an extremum at the symmetrical point for a symmetrical reaction coordinate. Except for the equilibrium structure of $HO-CH_2$ radical, both sides of the stationary points for the rotational coordinates of the radicals examined in the present work are symmetrical to each other. Thus, as matters of logical outcomes, μ and η both go through extrema at these stationary points. Noteworthy is that the behavior is not necessarily in accord with Datta's corollary. For example, for H_2N-CH_2 radical, η at the rotational TS is the maximum instead of the minimum (see Figure 5). Moreover, for H_2B-CH_2 radical, η goes through the minimum in two other structures rather than the TS (see Figure 3).

3.6. Polarizability. In similar to profiles of η, the variation of polarizability along a reaction coordinate is frequently discussed: a state of minimum polarizability is usually associated with that of maximum η.[18,19,25,27,29,37] Moreover, a quantitative relation between polarizability and η has been reported.[79−81] Thus, we computed the average molecular polarizability (α) for the rotational stationary points (see Table 6). For H_2N-CH_2 radical, the maximum η and the minimum η are associated with the rotational TS and the equilibrium structures, respectively. Correspondingly, the TS is lower in α than the equilibrium structure. For the H_2B-CH_2 radical, the minimum η is found for the structure with dihedral angle θ being around 50°, whose α is higher than those of the TS and the equilibrium structures. Furthermore, TS-1 has the maximum η for the $HO-CH_2$ radical, which corresponds to the observation that α is lower in TS-1 than in the equilibrium and the TS-2 structures. Nevertheless, in other cases, higher α is not necessarily associated with lower η. Similar observations have been reported for the rotamers of formamide and formthioamide: the magnitude of the average molecular polarizabilities of the rotamers is reversed from what expected from their η.[37]

There is no general relation between η and α for molecular systems, and the numerical results do not give any consistent trend. Thus, it may be premature to draw any concrete conclusion in the relationship between η and α. Even an equilibrium structure is not always associated with minimum polarizability, i.e., $\alpha_{TS} < \alpha_{eq.}$ in some cases.

4. Discussion

Comparing the behavior of η along the rotational coordinates with Datta's corollary is quite interesting. The feature of the variation of η of the H_3C-CH_2 radical is in accord with what expected from the corollary: the maximum and the minimum values of η are associated with the structures with the lowest and the highest potential energy, respectively. This is most likely to be related with the observation that the variation of μ of the H_3C-CH_2 radical is less than 0.5 kcal/mol: μ remains almost constant for the internal bond rotation of the H_3C-CH_2 radical. The other radicals undergo much larger variation of μ for the rotation. Thus, not surprisingly, the η profiles are not necessarily in accord with the corollary. For the H_2N-CH_2 radical, it is quite noteworthy that the η profile is completely opposite to that expected from the corollary: the rotational TS is associated with the maximum value of η and the equilibrium structure is associated with the minimum value of η. For the H_2B-CH_2 radical, the point of the minimum value of η is significantly deviated from the position of the rotational TS and that of the equilibrium structure. For the $HO-CH_2$ radical, although TS-2 is associated with the minimum value of η, the corollary also cannot be applied to the variation of η in the sense that the maximum value of η is not associated with the equilibrium structure but associated with TS-1.

To the best of our knowledge, a η profile that is opposed to Datta's corollary has not yet been reported for internal bond rotation. However, our investigations in the present work suggest that the features of η profiles for internal bond rotation of the substituted methyl radicals are not necessarily in accord with the corollary: except for the H_3C-CH_2 radical, an energetically more stable structure along the rotational coordinates is not always associated with higher η. In particular, the profiles of μ and η for internal bond rotation of the H_2N-CH_2 and $HO-CH_2$ radicals present striking contrast to those reported for internal bond rotation of closed-shell chemical species. Thus, we can safely conclude that there is no rigorous reason for η to be minimum in the TS region. This appears to be a quite natural conclusion, considering that the prerequisites of the PMH, i.e., constant μ and ν, cannot be satisfied all along the coordinate of a chemical process. Sannigrahi et al. pointed out a similar conclusion in their paper.[41] Furthermore, Jayakumar et al. pointed out in their recent work that η value is not applicable to prediction of the most stable structures of positional isomers.[82]

Bader[83] pointed out that a TS structure is usually accompanied by a low-lying excited state, which results in small HOMO−LUMO gap. A large number of observations[19−26,33−39] suggesting that Datta's corollary phenomenally holds in various chemical reactions appear to be more directly related with the presence of the low-lying excited state for the TS rather than the PMH.

5. Summary and Concluding Remarks

We have examined internal bond rotation of substituted methyl radicals, such as H_2B-CH_2, H_3C-CH_2, H_2N-CH_2, and $HO-CH_2$, and have investigated the rotational profiles of potential energy, electric chemical potential (μ), and hardness (η). The values of μ and η were calculated with three-point approximation, namely eqs 2a and 2b. The values of *IP* and *EA* were computed by performing separate energy evaluations for the neutral and its cationic and anionic species at the geometry of the neutral species. Geometry optimizations were carried out at B3LYP/6-31G(d) level, while energy evaluations were carried out with single-point B3LYP/6-311+G(2df,2p) and QCISD(T)/6-311+G(2df,2p) calculations at the B3LYP/6-31G-(d) optimized geometries. The computed rotational energy profiles, as well as the calculated values of the geometrical parameters, the vibrational frequencies, and the vertical/adiabatic ionization potentials, were in reasonable agreement with previously reported experimental and theoretical results.

On the basis of the principle of maximum hardness (PMH), Datta has introduced one interesting corollary: the transition state (TS) is likely to have a minimum value of η along a reaction coordinate.[15] The rotational η profile for H_3C-CH_2 radical is in accord with Datta's corollary: the maximum and the minimum values of η appear in the equilibrium and the TS structures, respectively. However, the η profile for H_2N-CH_2 radical is completely opposite to what expected from the corollary. The η profiles for H_2B-CH_2 and $HO-CH_2$ radicals are quite different from those expected from the corollary of the PMH. Thus, although there have been a large number of papers[19−26,33−39] suggesting that Datta's corollary phenomenally holds in various cases, we can safely conclude that there is no rigorous reason for η to be minimum in the TS region along a reaction coordinate. In addition, it is widely accepted that a state of higher η is usually associated with lower polarizability.[18,19,25,27,29,37] However, we have found several exceptional cases for H_2B-CH_2, H_3C-CH_2 and $HO-CH_2$ radicals where this relation does not hold.

Acknowledgment. The authors are grateful to Tsukuba Advanced Computing Center (TACC) and the Computer Center of National Institute of Materials and Chemical Research (NIMC) for generous allocation of computing time. A.K.C. is grateful to New Energy and Industrial Technology Development Organization (NEDO) for providing him a researcher position. Finally, the authors greatly appreciate highly suggestive and substantial comments of learned reviewers.

References and Notes

(1) Mulliken, R. S. *J. Am. Chem. Soc*. **1952**, *74*, 811−824.
(2) Pearson, R. G. *J. Am. Chem. Soc*. **1963**, *85*, 3533−3539.
(3) Pearson, R. G. *Science* **1966**, *151*, 172−177.
(4) Pearson, R. G. *Chemical Hardness*; Wiley-VCH: Weinheim, Germany, 1997.
(5) Donnelly, R. A.; Parr, R. G. *J. Chem. Phys*. **1978**, *69*, 4431−4439.
(6) Iczkowski, R. P.; Margrave, J. L. *J. Am. Chem. Soc*. **1961**, *83*, 3547−3551.
(7) Parr, R. G.; Pearson, R. G. *J. Am. Chem. Soc*. **1983**, *105*, 7512−7516.
(8) Yang, W.; Parr, R. G. *Proc. Natl. Acad. Sci. U.S.A.* **1985**, *82*, 6723−6726.
(9) Pearson, R. G. *J. Am. Chem. Soc*. **1985**, *107*, 6801−6806.
(10) (a) Pearson, R. G. *J. Chem. Educ.* **1987**, *64*, 561−567. (b) Pearson, R. G. *J. Chem. Educ.* **1999**, *26*, 267−275.
(11) Parr, R. G.; Chattaraj, P. K. *J. Am. Chem. Soc*. **1991**, *113*, 1854−1855.
(12) Parr, R. G.; Gazquez, J. L. *J. Phys. Chem*. **1993**, *97*, 3939−3940.
(13) (a) Pearson, R. G. *Acc. Chem. Res*. **1993**, *26*, 250−255. (b) Parr, R. G.; Zhou, Z. *Acc. Chem. Res*. **1993**, *26*, 256−258.
(14) Pearson, R. G.; Palke, W. E. *J. Phys. Chem*. **1992**, *96*, 3283−3285.
(15) Datta, D. *J. Phys. Chem*. **1992**, *96*, 2409−2410.
(16) Pal, S.; Vaval, N.; Roy, R. *J. Phys. Chem*. **1993**, *97*, 4404−4406.
(17) Chattaraj, P. K.; Nath, S.; Sannigrahi, A. B. *Chem. Phys. Lett.* **1993**, *212*, 223−230.
(18) Chattaraj, P. K.; Fuentealba, P.; Jaque, P.; Toro-Labbe, A. *J. Phys. Chem. A* **1999**, *103*, 9307−9312.
(19) Ghanty, T. K.; Ghosh, S. K. *J. Phys. Chem. A* **1996**, *100*, 12295−12298.
(20) Chattaraj, P. K.; Sannigrahi, A. B. *J. Phys. Chem*. **1994**, *98*, 9143−9145.
(21) Cardenas-Jiron, G. I.; Gutierrez-Oliva, S.; Melin, J.; Toro-Labbe, A. *J. Phys. Chem. A* **1997**, *101*, 4621−4627.
(22) Kar, T.; Schener, S.*J. Phys. Chem*. **1995**, *99*, 8121−8124.
(23) Mineva, T.; Sicilia, E.; Russo, N. *J. Am. Chem. Soc.* **1998**, *120*, 0, 9053−9058.
(24) Nath, S.; Sannigrahi, A. B.; Chattaraj, P. K. *J. Mol. Struct. (THEOCHEM)* **1994,** *309*, 65−77.
(25) Jaque, P.; Toro-Labbe, A. *J. Phys. Chem. A* **2000**, *104* 995−1003.
(26) Perez, P.; Toro-Labbe, A. *J. Phys. Chem. A* **2000**, *104* 1557−1562.
(27) Nguyen, L. T.; Le, T. N.; De Proft, F.; Chandra, A. K.; Langenaeker, W.; Nguyen, M. T.; Geerlings, P. *J. Am. Chem. Soc.* **1999**, *121*, 5992−6001.
(28) Nguyen. M. T.; Chandra, A. K.; Sakai, S.; Morokuma, K. *J. Org. Chem.* **1999**, *64*, 65−69.
(29) Le, T. N.; Nguyen, L. T.; Chandra, A. K.; De Proft, F.; Geelings, P.; Nguyen, M. T. *J. Chem. Soc., Perkin Trans. 2* **1999**, 1249−1255.
(30) Chandra, A. K.; Nguyen, M. T. *J. Phys. Chem. A* **1998**, *102*, 6181−6185.
(31) Sola, M.; Toro-Labbe, A. *J. Phys. Chem. A* **1999**, *103* 8847−8852.
(32) Subramanian, V.; Sivanesan, D.; Amutha, R.; Padmanabhan, J.; Ramasami, T. *Chem. Phys. Lett.* **1998**, *294*, 285−291.
(33) Chandra, A. K. *J. Mol. Struct. (THEOCHEM)* **1994**, *312*, 297−303.
(34) Cardenas-Jiron, G.; Lahsen, J.; Toro-Labbe, A. *J. Phys. Chem*. **1995**, *99*, 5325−5330.
(35) Cardenas-Jiron, G.; Toro-Labbe, A. *J. Phys. Chem*. **1995**, *99*, 12730−12738.
(36) Cardenas-Jiron, G.; Toro-Labbe, A.*J. Mol. Struct. (THEOCHEM)* **1997**, *390*, 79−89.
(37) Ghanty, T. K.; Ghosh, S. K. *J. Phys. Chem. A* **2000**, *104*, 2975−2979.
(38) Aliste, M. P. *J. Mol. Struct. (THEOCHEM)*, **2000**, *507*, 1−10.
(39) Kolandaivel, P.;Jayakumar, N. *J. Mol. Struct. (THEOCHEM)*, **2000**, *507*, 197−206.
(40) Pal, S.; Chandra, A. K.; Roy, R. K. *J. Mol. Struct, (THEOCHEM)* **1996**, *361*, 57−61.
(41) Kar, T.; Scheiner, S.; Sannigrahi, A. B. *J. Phys. Chem. A* **1998**, *102*, 5967−5973.
(42) Becke, A. D.*J. Chem. Phys.* **1993**, *98*, 5648−5652.
(43) For Quadratic CI calculations including single and double substitutions with a triples contribution to the energy, see: Pople, J. A.; Head-Gordon, M.; Raghavachari, K. *J. Chem. Phys.* **1987**, *87*, 5968−5975.
(44) Chen, W.; Schlegel. H. B. *J. Chem. Phys.* **1994**, *101*, 5957−5968**.**
(45) Hase, W. L.; Schlegel, H. B.; Balbyshev, V.; Page, M. *J. Phys. Chem.* **1996**, *100*, 5354−5361.
(46) Wittbrodt, J. M.; Schlegel, H. B. *J. Chem. Phys.* **1996**, *105*, 6574−6577.
(47) Durant, J. L. *Chem. Phys. Lett.* **1996**, *256*, 595−602.
(48) Mayer, P. M.; Parkinson, C. J.; Smith, D. M.; Radom, L. *J. Chem. Phys.* **1998**, *108*, 604−615.
(49) (a) Bauschlicher, C. W., Jr.*Chem. Phys. Lett.* **1995**, *246*, 40−44. (b) Ricca, A.; Bauschlicher, C. W., Jr. *J. Phys. Chem.* **1994**, *98*, 12899−12903. (c) Ricca, A.; Bauschlicher, C. W., Jr. *J. Phys. Chem*. **1995**, *99*, 5922−5926. (d) Ricca, A.; Bauschlicher, C. W., Jr. *J. Phys. Chem.* **1995**, *99*, 9003−9007.
(50) Vereecken, L.; Peeters, J. *J. Phys. Chem. A* **1999**, *103*, 1768−1775.
(51) Ihee, H.; Zewail, A. H.; Goddard, W. A. III *J. Phys. Chem. A* **1999**, *103*, 6638−6649.
(52) Kar, T.; Scheiner, A.; Sannigrahi, A. B. *J. Mol. Struct (THEOCHEM)* **1998**, *427*, 79−85.
(53) Roy, R. K.; Pal, S. *J. Phys. Chem.* **1995**, *99*, 17822−17824.

(54) De Proft, F.; Langenaeker, W.; Geerlings, P. *J. Phys. Chem.* **1993**, *97*, 1826−1831.
(55) Frisch, M. J.; Trucks, G. W.; Schlegel, H. B.; Scuseria, G. E.; Robb, M. A.; Cheeseman, J. R.; Zakrzewski, V. G.; Montgomery, J. A.; Stratmann, R. E.; Burant, J. C.; Dapprich, S.; Millam, J. M.; Daniels, A. D.; Kudin, K. N.; Strain, M. C.; Farkas, O.; Tomasi, J.; Barone, V.; Cossi, M.; Cammi, R.; Mennucci, B.; Pomelli, C.; Adamo, C.; Clifford, S.; Ochterski, J.; Petersson, G. A.; Ayala, P. Y.; Cui, Q.; Morokuma, K.; Malick, D. K.; Rabuck, A. D.; Raghavachari, K.; Foresman, J. B.; Cioslowski, J.; Ortiz, J. V.; Stefanov, B. B.; Liu, G.; Liashenko, A.; Piskorz, P.; Komaromi, I.; Gomperts, R.; Martin, R. L.; Fox, D. J.; Keith, T.; Al-Laham, M. A.; Peng, C. Y.; Nanayakkara, A.; Gonzalez, C.; Challacombe, M.; Gill, P. M. W.; Johnson, B. G.; Chen, W.; Wong, M. W.; Andres, J. L.; Head-Gordon, M.; Replogle, E. S.; Pople, J. A. GAUSSIAN98, Revision A.b; Gaussian, Inc.: Pittsburgh, PA, 1998.
(56) Suter, H. U.; Ha, T.-K. *Chem. Phys.* **1991**, *154*, 227−236.
(57) Ruscic, B. Berkowitz, J.; Curtiss, L. A. Pople, J. A. *J. Chem. Phys*. **1989**, *91*, 114−121.
(58) Pacansky, J.; Koch, W.; Miller, M. D. *J. Am. Chem. Soc.* **1991**, *113*, 3, 317−328.
(59) Jursic, B. S. *J. Phys. Chem. A* **1998**, *102*, 9255−9260.
(60) Curtiss, L. A.; Kock, L. D.; Pople, J. A. *J. Chem. Phys.* **1991**, *95*, 4040−4043.
(61) Bruna, P. J.; Grein, F. *J. Phys. Chem. A* **1999**, *102*, 3141−3150.
(62) Johnson, R. D. III; Hudgens, J. W. *J. Phys. Chem. A* **1996**, *100*, 19874−19890.
(63) Bauschlicher, C. W., Jr.; Prtridge, H. *Chem. Phys. Lett*. **1993**, *215*, 451−454.
(64) Glauser, W. A.; Koszykowski, M. L. *J. Chem. Phys.* **1991**, *95*, 10705−10713.
(65) Scott, A. P.; Radom, L. *J. Phys. Chem.* **1996**, *100*, 16502−16513.
(66) Coolidge, M. B.; Borden, W. T. *J. Am. Chem. Soc.* **1988**, *110*, 2298−2299.
(67) Pacansky, J.; Dupuis, M.*J. Chem. Phys.* **1978**, *68*, 4276−4278.
(68) Claxton, T. A.; Graham, A. M. *J. Chem. Soc., Faraday Trans 2* **1987**, *83*, 2307−2317.
(69) Peeters, D.; Lrroy, G.; Matagne, M.*J. Mol. Struct. (THEOCHEM)* **1988**, *166*, *267*−*277*.
(70) East, A. L. L.; Bunker, P. R. *Chem. Phys. Lett.* **1998**, *282*, 49−53.
(71) Pacansky, J.; Coufal, J. *J. Chem. Phys.* **1980**, *72*, 5285−5286.
(72) Sears, T. J.; Johnson, P. M.; Jin, P.; Oatis, S.*J. Chem. Phys.* **1996**, *104*, 781−792.
(73) Krusic, P. J.; Meakin, P.; Jessen, J. P. *J. Phys. Chem.* **1971**, *75*, 5, 3438−3453.
(74) Bauschlicher, C. W., Jr.; Partridge, H. *J. Phys. Chem*. **1994**, *98*, 1826−1829.
(75) Brinck, T.: Lee, H.-N.; Jonsson, M.*J. Phys. Chem. A* **1999**, *103*, 7094−7104.
(76) Froese, R. D. J.; Humbel, S.; Svensson, M.; Morokuma, K. *J. Phys. Chem. A* **1997**, *101*, 227−233.
(77) For most of the cases, the closed-shell singlet states of the cationic and anionic species were found to be lower in energy than the corresponding triplet or open-shell singlet states. Only for B3LYP calculations of anionic $H_2B-CH_2^-$ species at the geometries of θ being 80 and 90°, the open-shell singlet biradical states were found to be lower in energy than the closed-shell singlet states.
(78) Chandra, A. K.; Uchimaru, T. *J. Phys. Chem. A.* **2001**. Submitted for publication.
(79) Hati, S.; Datta, D. *J. Phys. Chem.* **1994**, *98*, 10451−10454.
(80) Roy, R. K.; Chandra, A. K.; Pal, S. *J. Mol. Struct. (THEOCHEM)* **1995**, *331*, 261−265.
(81) Hohm, U. *J. Phys. Chem. A* **2000**, *104*, 8418−9423.
(82) Jayakumar, N.; Kolandaivel, P. *Int. J. Quantum Chem.* **2000**, *76*, 648−655.
(83) Bader, R. F. W. *Can. J. Chem.* **1962**, *40*, 1164−1175.
(84) Pople, J. A.; Apeloig, Y.; Schleyer, P. von, R. *Chem. Phys. Lett.* **1982**, *85*, 489−492.
(85) Pacansky, J.; Dupuis, M.; *J. Am. Chem. Soc.* **1982**, *104*, 415−421.
(86) Jacox, M. E.; Milligan, D. *J. Mol. Spectrosc*. **1973**, *47*, 148−162.
(87) Jacox, M. E. *Chem. Phys.* **1981**, *59*, 213−230.
(88) Berkowitz, J.; Ellison, G. B.; Gutman, D. *J. Phys. Chem.* **1994**, *98*, 8, 2744−2765.
(89) Dyke, J. M.; Ellis, A. R.; Keddar, N.; Morris, A. *J. Phys. Chem.* **1984**, *88*, 8, 2565−2569.
(90) Rosenstock, H. M.; Buff, R.; Ferreira, M. A. A.; Lias, S. G.; Parr, A. C.; Stockbauer, R. L.; Holmes, J. L. *J. Am. Chem. Soc*. **1982**, *104*, 2337−2345.
(91) Dyke, J. M.; Lee, E. P. E.; Niavaran, M. H. Z.*Int. J. Mass Spectrom. Ion Processes* **1989**, *94*, 221−235.
(92) Masaki, A.; Tsunashima, S.; Washida, N. *J. Phys. Chem.* **1995**, *99*, 9, 13126−13131.
(93) Dyke, J. M. *J. Chem. Soc., Faraday Trans. 2* **1987**, *83*, 69−87.
(94) Riscic, B.; Berkowitz, J. *J. Chem. Phys.* **1991**, *95*, 4033−4039.
(95) Tao, W.; Klemm, R. B.; Nesbitt, F. L.; Stief, L. J. *J. Phys. Chem.* **1992**, *96*, 104−107.